RSC Advances

PAPER

View Article Online
View Journal | View Issue

Cite this: *RSC Adv.*, 2020, **10**, 21057

Dityrosine suppresses the cytoprotective action of thyroid hormone T3 *via* inhibiting thyroid hormone receptor-mediated transcriptional activation†

Yin-Yi Ding, ‡*[ab] Fang-Fang Wang,‡[c] Yu-Ge Jiang,[de] Yi-Jing Sheng,[a] Meng-Qi Jiang,[a] Xuan Zhu,[a] Yong-Hui Shi[de] and Guo-Wei Le [de]

Received 10th January 2020
Accepted 18th May 2020

DOI: 10.1039/d0ra00276c

rsc.li/rsc-advances

Dityrosine (Dityr) is the most common oxidized form of tyrosine. In the previous studies of mice treated with dityrosine, cell death in the pancreas, kidneys, and liver was detected in the presence of enhanced plasma triiodothyronine (T3) content. Due to its structural similarity with the thyroid hormone T3, we hypothesized that dityrosine might disrupt T3-dependent endocrine signaling. The cytotoxic effect of dityrosine was studied in C57BL/6 mice by gavage with a dityrosine dose of 320 μg per kg per day for 10 weeks. Cell death in the liver was detected in the presence of enhanced plasma thyroid hormone content in mice treated with dityrosine. The antagonistic effect of dityrosine on T3 biofunction was studied using HepG2 cells. Dityrosine incubation reduced T3 transport ability and attenuated the T3-mediated cell survival *via* regulation of the PI3k/Akt/MAPK pathway. Furthermore, dityrosine inhibited T3 binding to thyroid hormone receptors (TRs) and suppressed the TR-mediated transcription. Dityrosine also downregulated the expressions of T3 action-related factors. Taken together, this study demonstrates that dityrosine inhibits T3-dependent cytoprotection by competitive inhibition, resulting in downstream gene suppression. Our findings offer insights into how dityrosine acts as an antagonist of T3. These findings shed new light on cellular processes underlying the energy metabolism disorder caused by dietary oxidized protein, thus contributing to a better understanding of the diet–health axis at a cellular level.

1. Introduction

Some food ingredients, such as oxidized protein in protein-rich processed food, can affect glucose and lipid metabolism by disrupting physiological processes, particularly through direct or indirect interaction with thyroid hormones.[1] Recent public and scientific interest has been mostly focused on protein oxidation in food systems during food processing and storage[2] and the effects of dietary oxidized protein on human health.[3] During food processing and storage, proteins are vulnerable to oxidation by both radical and non-radical oxidant factors,[4] such as tyrosine, being readily oxidized to dityrosine (Dityr).[5] Dityrosine, which exhibits pro-oxidant behavior, is considered an endocrine disruptor[6] that causes oxidative damage in the liver[7] and kidneys.[8] Exposure to dityrosine changes many systemic metabolic processes, including reduced choline bioavailability as well as cell death in the liver, kidneys, and pancreas.[9–12] Dityrosine exposure also induces learning and memory impairments.[13,14] The endocrine disrupting effects of dityrosine are seen in other nuclear receptors, such as thyroid hormone receptors (TRs), acting as an antagonist to triiodothyronine (T3).[15]

T3 is widely known for the ability to influence various cellular processes,[16] energy expenditure, and metabolic rate.[17,18] Numerous of studies have documented that T3 is a survival factor in cells, counteracting both physiological and pharmacological cell death.[19] Evidence of protein–protein interactions between cytosolic TRs and phosphatidylinositol 3-kinase (PI3K) as well as activation of PI3K activity by T3 treatment have been reported.[20,21] T3 can directly stimulate the activation of Akt, and activate cellular processes strictly related to cell function such as cell proliferation and survival, cell size regulation, protein synthesis, and insulin production.[22,23] Thyroid hormone receptor β1 (TRβ1) mediates T3 upregulation of protein synthesis and cell survival playing a crucial role in T3 regulation of the PI3K/Akt pathway.[24] TRβ1 seems to be an essential component in mediating T3 action on Akt pathway in the

[a]*Collage of Food Science and Biotechnology, Zhejiang Gongshang University, No.18, Xuezheng Street, Hangzhou, 310018, China. E-mail: dyy-198655@163.com; Fax: +86 571-28877777; Tel: +86 571-28877777*

[b]*Food Nutrition Science Centre, Zhejiang Gongshang University, Hangzhou, 310018, China*

[c]*School of Life Science, Linyi University, Linyi, 276000, China*

[d]*The State Key Laboratory of Food Science and Technology, Jiangnan University, Wuxi, 214122, China*

[e]*Center of Food Nutrition and Functional Food Engineering, School of Food Science and Technology, Jiangnan University, Wuxi, 214122, China*

† Electronic supplementary information (ESI) available. See DOI: 10.1039/d0ra00276c

‡ Yin-Yi Ding and Fang-Fang Wang contributed equally.

pancreas.[24,25] We previously demonstrate that the increase of TRβ1 protein level induced by T3 is significantly inhibited by dityrosine, which subsequently suppress the T3-induced phosphorylation of Akt.[15] Taken together, these results suggest that dityrosine may act as an antagonist in T3-regulated cell survival.

The structures of dityrosine and T3 are shown in Fig. 1. The resemblance between dityrosine and T3 is high at 70% similarity according to the database of Chemical Entities of Biological Interest (ChEBI, http://www.ebi.ac.uk/chebi/). Because of its structure homology with T3, the thyroid endocrine system disrupted by dityrosine is studied. Previous studies in our laboratory found that dityrosine administration disrupts regulation of the thyroid hormone T3 by targeting glucose-stimulated insulin synthesis in the pancreas.[1] Furthermore, thyroid hormone receptor β1 (TRβ1) and translational factors involved in Akt-mTOR signaling pathway are modulated by dityrosine.[15]

T3 binds to TRs and then binds to a target DNA sequence known as a thyroid hormone response elements (TRE), composed of two half-site core motifs (AGGTCA) with specific nucleotide spacing and orientation.[26,27] Besides, RAR-related orphan receptors α (RORα) is a novel member of the nuclear hormone receptor superfamily. Although the ligand of RORα has not been identified and its bio-function is not clear, RORα is widely expressed, including in central nervous system.[28] RORα binds to a hormone-response element (ROR-response element [RORE]), which is composed of a 6-bp AT-rich sequence 5′, a half core motif (GGTCA), and an active transcription.[28] As TRs and RORα are transcription factors that share a common core motif within the response elements, previous studies have demonstrated that RORα modulates TRs action on TRE by competitively binding to the TRE and forming heterodimers with the TRs.[29]

Given the findings of the aforementioned researches, examining the relationship between dityrosine and T3 action is at present a major research topic. However, previous studies have not fully explained the antagonistic effects and mechanisms of dityrosine on T3 action. In the present study, we investigate the effects of dityrosine on the cytoprotection action of T3 in liver *via* a 10 week gavage experiment involving C57BL/6 mice administrated with dityrosine. We used molecular docking simulations to determine the effects of dityrosine on the TRβ1–T3 binding ability. Moreover, we performed T3–TRβ1 binding studies using [^{125}I]T3 to determine the effects of dityrosine on the T3–TRβ1 binding ability. Finally, we conducted a cell experiment exposing HepG2 cells to dityrosine and T3 to evaluate whether dityrosine could suppress T3 action and investigated the effects of dityrosine on the crosstalk between TRs and T3 on TRE *via* a transient transfection study.

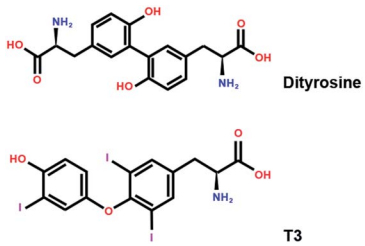

Fig. 1 The chemical structure of T3 and dityrosine.

2. Materials and methods

2.1. Animal experiment using C57BL/6 mice

2.1.1. Animals and dityrosine dose. Four-week-old male C57BL/6 mice were purchased from Model Animal Research Center of Nanjing University. Mice were housed in a temperature-controlled room at 24 ± 2 °C with a 12 h light–dark cycle (Research animal center of Zhejiang Gongshang University). The mice were feed with standard feed. The compositions of standard diets are shown in ESI Table 1.†

We previously performed a 6 week preliminary study and found that gavage with a dityrosine dose of 320 μg per kg per day caused thyroid hormone resistance and novel object recognition deficits in C57BL/6 mice.[15,29] In this study, mice were randomly divided into two groups that received either dityrosine (Ruidong Biotechnology, Shanghai, China; dityrosine > 95%) (Dityr group) or saline solution (control group) ($n = 10$) after 7 days of acclimatization. After a 10 week period, the mice were anesthetized by pentobarbital sodium (50 mg kg^{-1}, i.p.). Blood was collected from the orbital sinuses and placed into anticoagulant tubes. Plasma was obtained from the blood samples after centrifugation (1570×g for 10 min at 4 °C). All mice were sacrificed by cervical dislocation. The liver was dissected by an animal care technician based on morphological features and fixed in 10% formaldehyde phosphate buffer. The rest of the liver was rinsed with saline and flash frozen in liquid nitrogen for further analysis.

All animal treatments were performed in accordance with the ethical standards set by the National Institutes of Health Guide for the Care and Use of Laboratory Animals (China) and in the 1964 Declaration of Helsinki and its later amendments. All animal studies were approved by the Laboratory Animals Ethics Committee of Zhejiang Gongshang University.

2.1.2. Measurements of total/free T4 (TT4 and FT4), total/free T3 (TT3 and FT3), and insulin levels in plasma. Plasma levels of TT4, FT4, TT3, and FT3 were measured using the ELISA kits (Huijia Biotechnology; China) according to manufacturer's instruction.

2.1.3. Histopathological analysis. The liver was fixed in 10% formaldehyde phosphate buffer for 24 h, and embedded in paraffin. Haematoxylin and eosin (H–E) staining was performed on 5 μm serial sections to analyze histopathological changes. Cell apoptosis was determined by terminal deoxynucleotidyl transferase dUTPnick end labelling (TUNEL) staining (Beyotime Biotechnology; China). Images of slices were taken with an optical microscope (BX41, Olympus, Japan) and analyzed using the Image-Pro Plus 5.0 software (Media Cybernetics, Inc.; USA).

2.1.4. Immunohistochemistry (IHC) analysis. The 5 μm thick paraffin sections were deparaffinized and rehydrated with a series of xylene and aqueous alcohol solutions, respectively. After antigen retrieval in ethylenediaminetetraacetic acid (EDTA, pH 9.0) for 8 min, the slices were washed with PBS

(0.01 M, pH 7.4) and incubated with 3% H_2O_2 solution to block the endogenous peroxidase at room temperature in a dark environment for 25 min. The slices were washed with PBS (0.01 M, pH 7.4) and incubated with 1% bovine plasma albumin for 1 h. The locking plasma was tapped off, and the slices were incubated with primary antibody against caspase 3 (1 : 500) (Servicebio, China) at 4 °C overnight. The slices were subsequently incubated with horseradish peroxidase-conjugated secondary antibody (1 : 200) (Servicebio, China) for 30 min at 37 °C. DAB coloration kit (DAKO, Denmark) was used for color-reaction. Slices were counterstained with hematoxylin. The pictures of the slices were taken by optical microscope (BX41, Olympus, Japan). The immunostaining intensity was analyzed using the Image-pro Plus 5.0 software (Media Cybernetics Inc., USA).

2.2. Cell experiment using HepG2 cells

2.2.1. Culture and cell treatment. HepG2 cells were purchased from the cell bank at the Type Culture Collection of Chinese Academy of Sciences (Shanghai; China) and grown in Dulbecco's Modified Eagle Medium (DMEM) supplemented with 4.0 mM glucose and 10% foetal bovine serum (FBS) (Gibco; USA).

The cells were seeded in plates and permitted to adhere at 37 °C in a humidified atmosphere containing 95% O_2 and 5% CO_2 for 24 h. When the cells reached 40% confluence, they were stimulated with dityrosine (final concentration: 0, 0.1, 1, or 10 μM) or T3 (final concentration: 0 or 1 μM for 72 h).

2.2.2. Measurement of cellular T3 level in HepG2 cells. HepG2 cells were lysed on ice using RIPA Lysis Buffer (P0013B, Beyotime Institute of Biotechnology; China) at the end of the incubation. Lysates were transferred to sterilized tubes and centrifuged to obtain the supernatant (1570×*g*, 10 min at 4 °C). T3 level in the supernatant was measured by T3 ELISA kit (Huijia Biotechnology; China).

2.2.3. Cell viability assay. At the end of the treatment, MTT (0.5 mg mL^{-1}) was added to each well for 4 h. Subsequently, medium and MTT were removed, and precipitate was dissolved with DMSO. The optical density was measured at 570 nm with a Mutiskan Spectrum (Epoch, BioTek, Vermont, U.S.A.).

2.3. Protein extracts and western blot analysis

Protein was extracted from HepG2 cells using RIPA Lysis Buffer containing 50 mM Tris (pH 7.4), 150 mM NaCl, 1% Triton X-100, 1% sodium deoxycholate, 0.1% SDS and protease inhibitors (sodium orthovanadate, sodium fluoride, EDTA and leupeptin). One mM (final concentration) phenylmethanesulfonyl fluoride was added to the lysis buffer before use. Liver (200 mg) and cells were homogenized in 1.5 mL lysis buffer on ice. After lysis, the homogenate was centrifuged for 5 min at 12 000×*g*. The protein concentration in the supernatant was determined by the BCA assay kit (Nanjing Jiancheng Bioengineering Institute, China) according to the manufacturer's instructions. All extracts were mixed with 1× loading buffer (50 mM Tris–HCl pH 6.8, 100 mM dithiothreitol, 2% SDS, 0.1% bromophenol blue, 10% glycerol and 5% β-mercaptoethanol) in the ratio of 4 : 1 and then were boiled at 95 °C for 10 min to denature the protein.

The proteins were separated by 12% SDS-PAGE gel with 10 μg of total protein per lane and then transferred onto nitrocellulose membrane. The membranes were blocked in Tris-buffered saline (pH 7.4) with 5% bovine serum albumin (BSA) and 0.1% Tween 20. The blocked membrane was incubated with the following primary antibody: rabbit TRβ1, MAPK (ERK1/2), phosphor-MAPK (ERK1/2) (Thr202/Tyr204), caspase 3, Bax, Bcl-2 antibody and rabbit β-actin antibody (1 : 1000; Cell Signaling Technology; USA) at 4 °C for 10 h. The blots were incubated with secondary antibody (1 : 4000; Sigma-Aldrich, USA) and fluorescence images were obtained with an automatic chemiluminescence imaging analysis system (LI-COR Biosciences, USA).

2.4. Total mRNA isolation and quantitative RT-PCR (qRT-PCR)

Total RNA was extracted with Trizol reagent according to the manufacturer's protocol (Applied Biosystems; U.S.A.). qRT-PCR was performed using an SYBR green based qRT-PCR kit according to the manufacturer's instructions on a 7900HT instrument (Applied Biosystems, USA). The specificity of the product was assessed from melting curve analysis. Gene expressions were determined using the $2^{-\Delta\Delta CT}$ method. The primer's sequences for the genes are shown in ESI Table 2.†

2.5. Molecular docking simulations

Molecular docking simulations of the ligands (dityrosine and T3) into the TRβ1 (1NAX) binding sites were performed using AutoDock (version 4) in the present work,[30] the crystal structures of 1NAX were extracted from the Protein Data Bank (http://www.rscb.org/pdb). The grid-based docking program was used to obtain the binding modes of the compounds. The interaction energy between the ligands and TRβ1 were evaluated using atom affinity potentials calculated on a grid similar to the one described by Goodford.[31] During the molecular docking process, the molecule in the crystal structure was used as a standard docking model.

For molecular docking, AutoGrid was used for preparing the grid map using a grid box with a docking box of 60 × 60 × 60 Å, the box spacing was set to 0.375 Å. The grid center was designated with the following dimensions (*xyz*): 9.421 × 16.953 × 26.432. The docking possibilities were calculated by the genetic algorithm with local search (GALS). For each ligand, the simulation was composed of 100 docking runs using the standard AutoDock parameters.

2.6. T3 binding study

2.6.1. Nuclei isolation from HepG2 cells. Nuclei were isolated from HepG2 cells as previously described.[32] Briefly, the cells were resuspended with precooled STME reagent (0.32 M sucrose, 20 mM Tris–HCl (pH 7.8), 1 mM $MgCl_2$, and 5 mM EDTA). The cells were lysed with 1× passive lysis buffer (PLB) and then centrifuged (1000×*g* for 10 min). The precipitate was

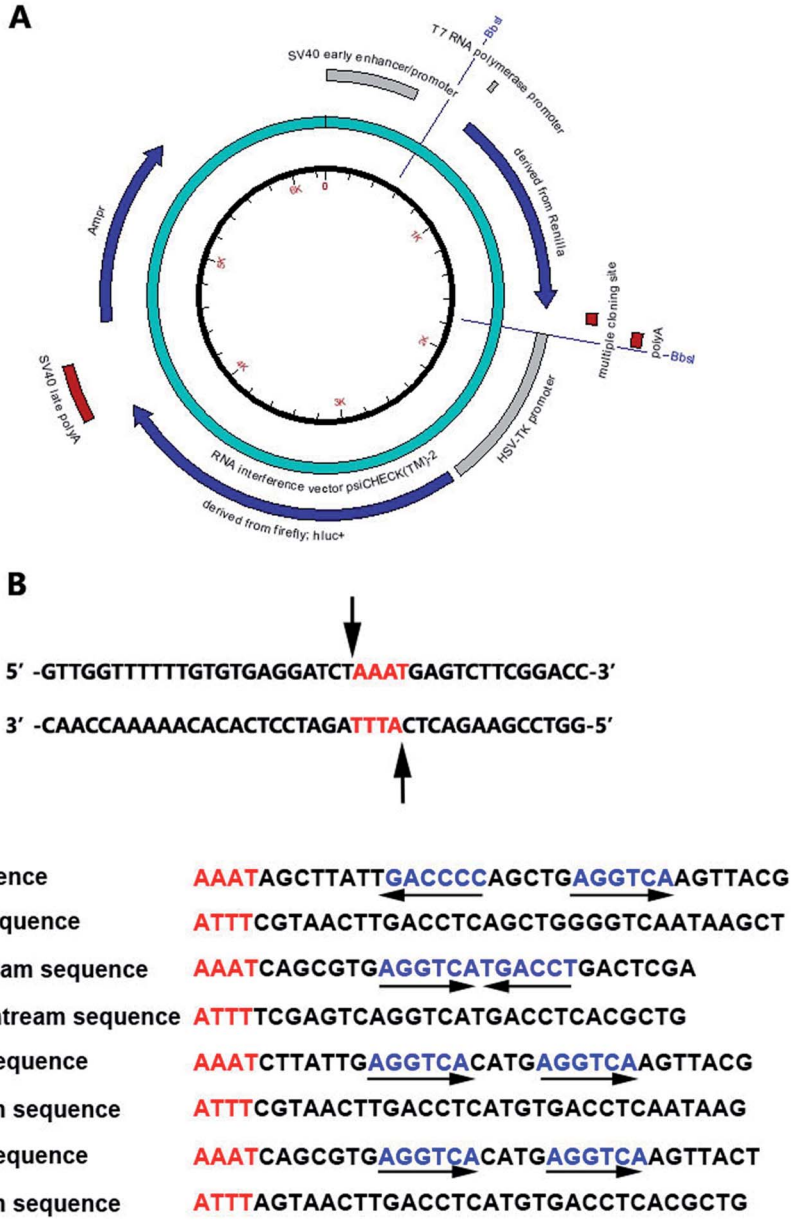

Fig. 2 (A) The reporter plasmids; (B) the cutting site; (C) the nucleotide sequences of double-stranded oligonucleotides containing TRE or RORE.

washed with Triton-X and STM reagent (STME reagent without EDTA).

2.6.2. Preparation of nuclear thyroid hormone receptors (TRs). Nuclear TRs were prepared from the purified nuclei as previously described.[32] Briefly, the nucleus was incubated in KMT reagent (200 mM Tris–HCl [pH 7.8], 0.4 M KCl, 1 mM $MgCl_2$, 5 mM dithiothreitol) for 45 min and then centrifuged (1000×*g* for 20 min). The supernatant was collected as the nuclear receptor extract. The total protein content was determined by the Lowry method.[33]

2.6.3. T3 binding studies using [^{125}I]T3. The T3 binding studies were performed according to Shafie,[34] with a few modification. Nuclear TRs and a tracer dose of [^{125}I]T3 in insulation medium (20 mM Tris–HCl [pH 7.8], 1 mM $MgCl_2$, 0.03% BSA, 5 mM dithiothreitol, and 0.32 M sucrose) were incubated with dityrosine at 4 °C for 2 h. Bound and free [^{125}I] T3 were separated by adding albumin dextran coated charcoal solution (ADCC) (3% charcoal (Norit, Netherlands), 2% BSA, 50 mM KCl, 50 mM KH_2PO_4–K_2HPO_4 (pH 7.85), and 0.3% dextran). The nonspecific binding value obtained in the presence of excess T3 was subtracted from the total binding value. The half-maximal inhibitory inhibition concentration (IC50) was calculated using Prism 7.0 software (GraphPad Software, U.S.A.).

2.7. TRs-mediated transcriptional activation

2.7.1. Design of oligonucleotides and plasmids. We designed the following oligonucleotides and plasmids according to the method of Koibuchi *et al.*[29] F2 (chick lysozyme TRE at

nucleotides −2358 to −2326; half-sites arranged as an inverted palindrome with nucleotide gap of 6 (ref. 35)); palindromic (typical TREs, which designed not to contain a putative RORE); DR4-1 (DR4 sequence containing AT-rich sequences at the 5′ end of the upstream half-site to serve as a putative RORE); and DR4-2 (DR4 oligonucleotide lacking an AT-rich sequence).[36] These oligonucleotides were cloned in the psi-CHECK2 vector (Thermo Fisher Scientific, USA) containing a viral thymidine kinase promoter coupled to the firefly luciferase-labelled gene which was used as the internal reference to remove the transfection efficiency differences between groups, and the *Renilla luciferase* reporter gene.[37] These reporter plasmids were sequenced to ensure that only a single copy of the TRE had been incorporated (Fig. 2A).

Accelrys DS Gene software (Accelrys Software, Inc., U.S.A.) was adopted to analyze the enzyme-cutting site of the psiCHECK2 promoter between the Poly A and hsv-tk promoter. The Bbs I enzyme was selected and the cutting site is shown in Fig. 2B. The nucleotide sequences of the double-stranded oligonucleotides containing TRE or RORE are shown in Fig. 2C.

2.7.2 Cell transfection assay. HepG2 cells were stimulated with dityrosine or T3 for 48 h. After the incubation, transfections were performed in strict accordance with the Lipofectamine® 3000 reagent kit instructions (Thermo Fisher Scientific, MA, USA). When cells reached 70% confluence, 100 μL of plasmid lipid complex was added to each well. Cells were subsequently incubated for 24 h.

2.7.3. Detection of dual-luciferase reporter gene activity. The protocol of dual-luciferase reporter gene activity detection was performed in strict accordance with the Promega kit instruction (Promega, WI, USA). The relative luciferase activity was determined by the ratio of *Renilla luciferase* activity to firefly luciferase activity (Renilla/Firefly).

2.8. Statistical analysis

All measurement value are expressed as mean ± S.E.M. Significant differences between groups were determined by one-way analysis of variance (ANOVA) using SPSS 20.0 software (IBM, Armonk, NY, USA) for Windows. Differences are considered significant at $p < 0.05$.

3. Results

3.1. Dityrosine causes histopathological changes and apoptosis in liver accompanied by increased THs level

As shown in Fig. 3A and B, at the morphological level, the liver of control mice showed normal hepatocellular architecture with the trabeculae of hepatocytes separated by blood sinusoids radiating from the central vein. The hepatocytes with mostly round or oval nuclei located on the side of the cell membrane were arranged with each other. The shapes of the cells were regular and the cell boundary were clear. The livers of dityrosine-treated mice showed improvement in the hepatocellular damage caused by dityrosine, including loss of architecture, unclear cell boundaries, and area of hepatocyte swelling, vacuolation and inflammation (leukocyte infiltration). In addition, dityrosine treatment resulted in a much higher number of TUNEL-positive cells compared to that in the control mice.

To deepen into the molecular changes induced by dityrosine in the apoptosis cascade, two major pro-apoptotic molecules and one anti-apoptotic molecule were analyzed by qRT-PCR. As shown in Fig. 4, dityrosine clearly induced the mRNA expression of *Bax* and *caspase 3*, and significantly decreased the expression of *Bcl-2*. However, TT3, FT4, and FT3 in plasma increased in dityrosine-treated mice (Fig. 5). These results showed that the cell death observed in livers of dityrosine-treated mice accompanied

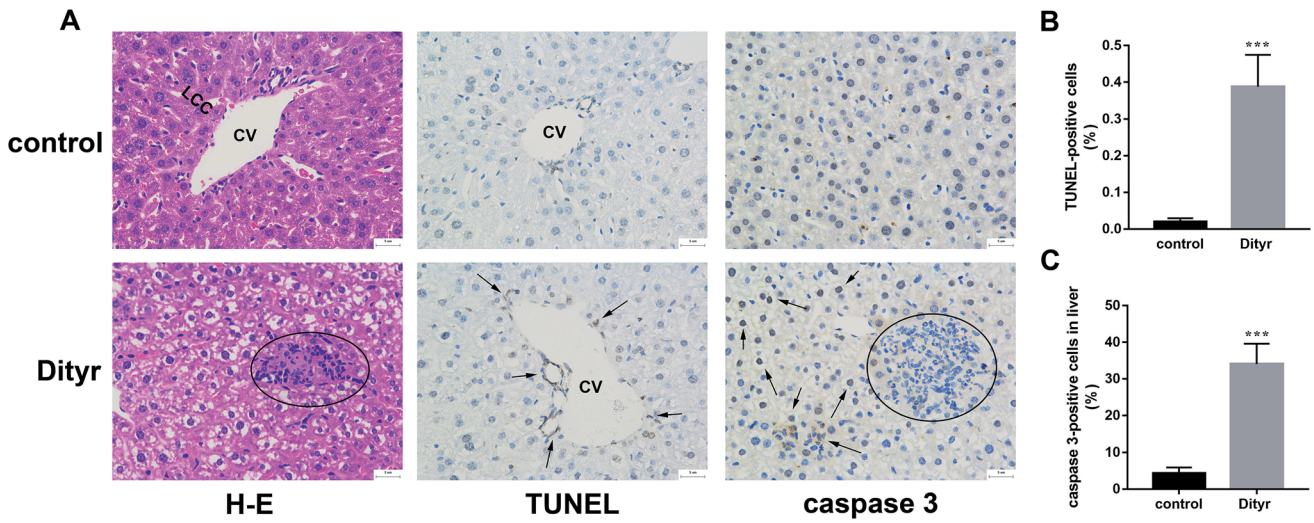

Fig. 3 Dityrosine causes apoptosis in liver of mice. (A) H & E staining image (first panel, 400×, space bar: 50 μm, the circle indicates inflammatory cell infiltration), the TUNEL staining image (second panel, 400×, space bar: 50 μm, the arrows indicate TUNEL-positive cells), the caspase 3 immunohistochemistry image (third panel, 400×, space bar: 50 μm, the circle indicates inflammatory cell infiltration, the arrows indicate caspase 3-positive cells); (B) the percentage of TUNEL-positive cells of liver (%); (C) the percentage of caspase 3-positive cells (%).***$p < 0.001$ when compared with the control group.

Fig. 4 The mRNA expression of Bax, caspase 3, and Bcl-2 of liver. ***$p < 0.001$ when compared with the control group.

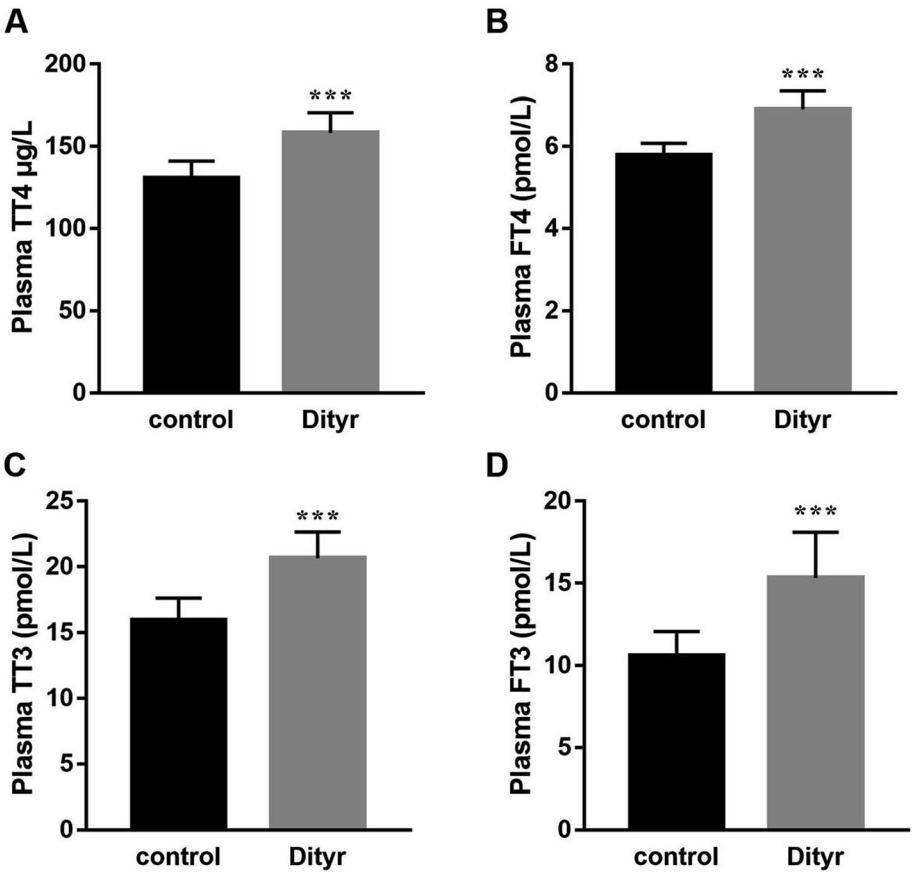

Fig. 5 Dityrosine changes the plasma content of THs. (A) Plasma TT4 content of mice; (B) plasma TT3 content of mice; (C) plasma FT4 content of mice; (D) plasma FT3 content of mice. ***$p < 0.001$ when compared with the control group.

by increased T3 level, which suggested that dityrosine administration might suppresses the cytoprotection action of T3.

3.2. Dityrosine suppresses T3-dependent survival of HepG2 cells

We used HepG2 cells as model to verify the hypothesis that cytoprotection action of T3 was disrupted by dityrosine as an antagonist. As shown in Fig. 6, dityrosine-only treatment caused a markedly increased degree of apoptosis in HepG2 cells, which was accompanied by alteration of the expression of apoptosis-related genes. Meanwhile, the survival of cells with 1 μM T3 treatment in the presence of dityrosine was notably declined when compared to cells exposed to T3 only.

As shown in Fig. 7, the western blot results confirmed that protein level of PI3k, the phosphorylation of Akt (Ser473/Thr308), and phosphorylation of MAPK (Thr202/Tyr204) increased when the cell were treated with only T3. Dityrosine exposure markedly declined the protein level of PI3k, p-Akt

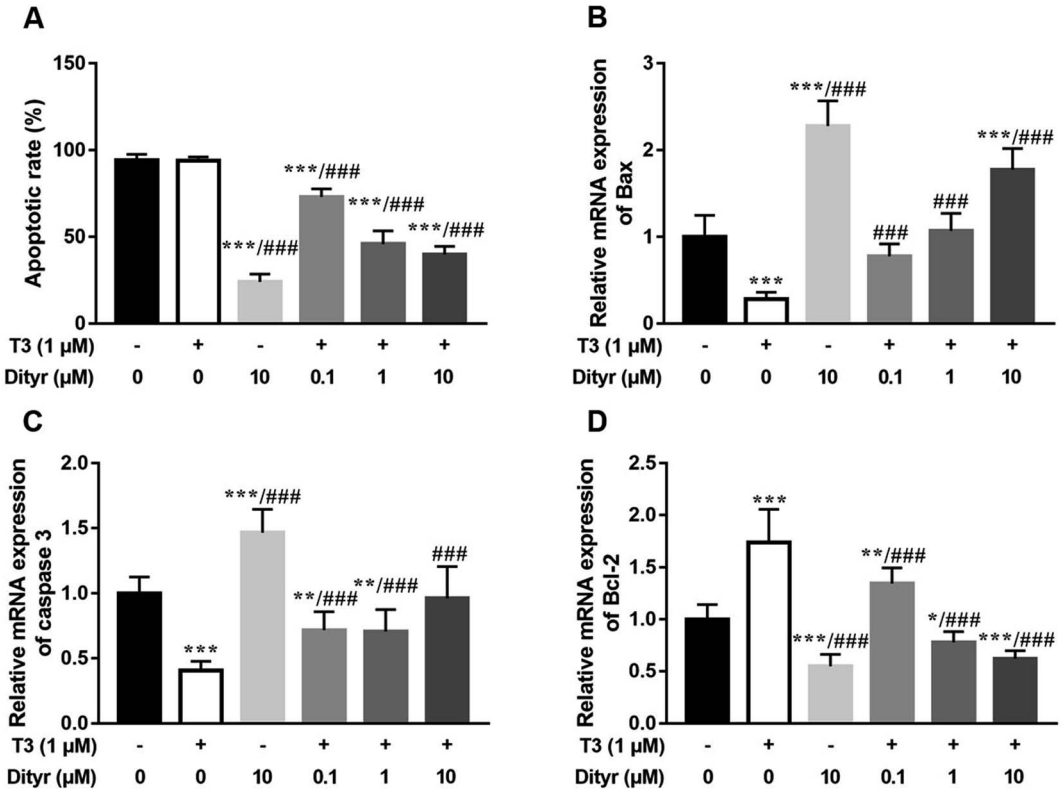

Fig. 6 Dityrosine causes apoptosis in HepG2 cells. (A) the proportion of apoptotic cells in each group evaluated by flow cytometry; (B–D) the mRNA expression of Bax, caspase 3, and Bcl-2. *$p < 0.05$, **$p < 0.01$, ***$p < 0.001$ when compared with the control group. ###$p < 0.001$ when compared with T3-only treated cells.

(Ser473/Thr308), and p-MAPK (Thr202/Tyr204). Meanwhile, the protein expressions of PI3k and phosphorylated Akt and MAPK induced by T3 were suppressed with the addition of dityrosine.

Together with our previous evidences in mice model in this paper, these results strongly suggested that dityrosine inhibited the T3-denpendent protective effects on cells at least in part through the PI3k/Akt/MAPK pathway and apoptotic cascade.

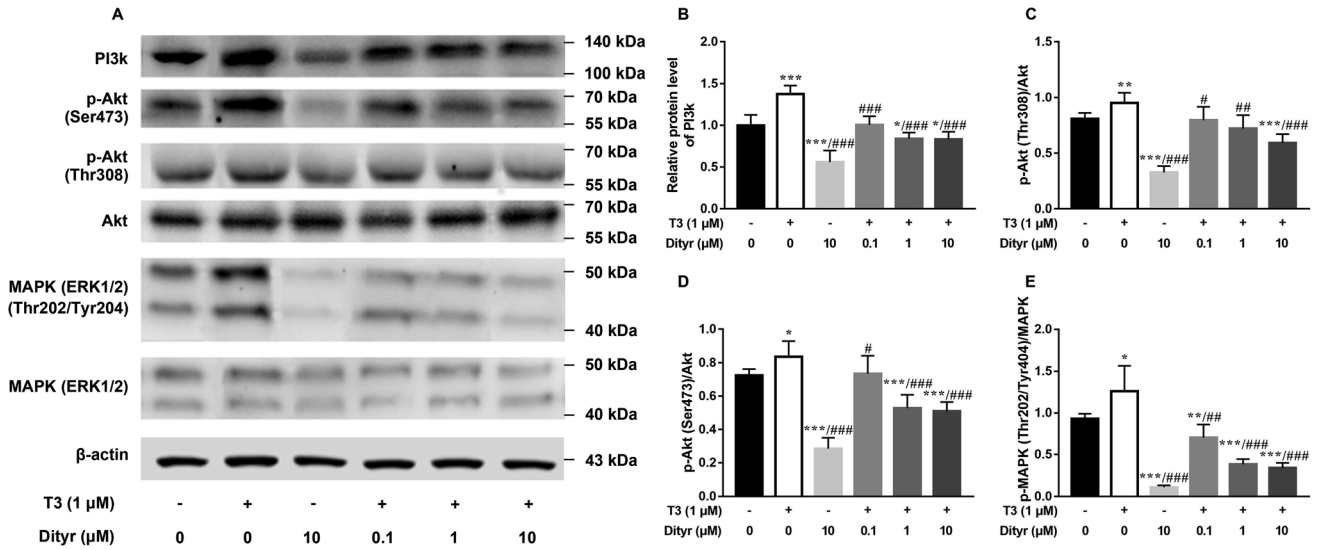

Fig. 7 Dityrosine suppresses the activity of PI3k/Akt/MAPK pathway. (A) The western blot image; (B) the quantitative result of the PI3k protein expression; (C and D) ratio of phosphorylated (Thr 308 and Ser 473) Akt and Akt; (E) ratio of phosphorylated (Thr 202/Tyr 404) MAPK and MAPK. *$p < 0.05$, **$p < 0.01$, ***$p < 0.001$ when compared with the control group. #$p < 0.05$, #$p < 0.01$, ###$p < 0.001$ when compared with T3-only treated cells.

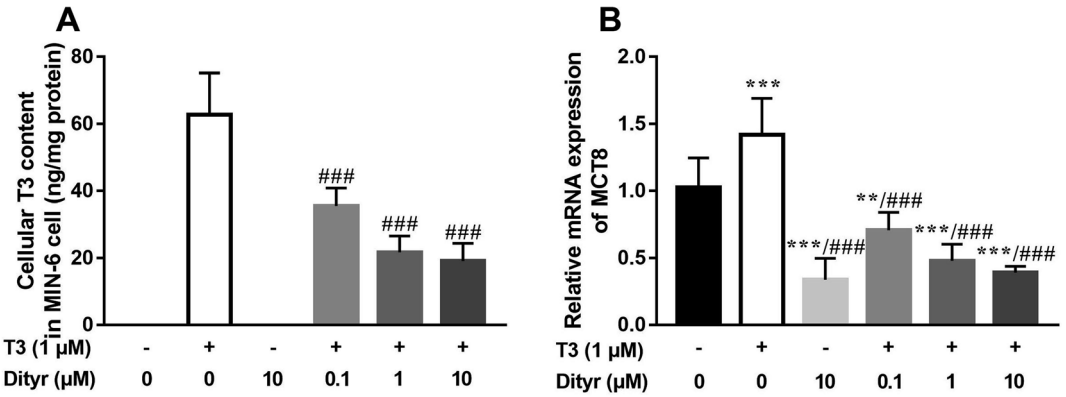

Fig. 8 Dityrosine reduces the transport ability of T3. (A) The cellular T3 concentration in MIN-6 cell; (B) the mRNA expression of MCT8. $^{**}p < 0.01$, $^{***}p < 0.001$ when compared with the control group. ###$p < 0.001$ when compared with T3-only treated cells.

3.3. Dityrosine reduces T3 transport and the expression of T3 action-related factors

As shown in Fig. 8A and B, the cellular T3 content and mRNA level of the T3 membrane transporter (MCT8) in dityrosine + T3-treated cells were significantly lower than those of the in cells treated with T3 only. These results suggested that T3 transport ability was suppressed by dityrosine.

3.4. Dityrosine and T3 competitively bind to TRβ1

To investigate the role of dityrosine in the function of T3, we determined the competitive inhibition of dityrosine on T3 action. A molecular docking study showed the protein–inhibitor interactions and the structural features of active site of the receptor. As with models of 1NAX-DT, the combine pocket of the receptor was exposed in Fig. 9A. Dityrosine was packaged in the pocket, which was composed by the residues Arg282, Leu341, Phe455, Phe269, Ser314, Gly345, Arg320, Phe272, Met442, Arg317, Gly344, Met313, Thr273, Ile275, Ile276, His435, Leu346, Ala279, Met310, and Arg316. Fig. 9B showed dityrosine had three hydrogen bond interactions with the receptor. The –COOH made two hydrogen bonds with the Arg282 (H-1, –O···HN, 151.4°) and Arg320 (H-2, –O···HN, 155.8°) amino acids at the distances of 2.11 Å and 2.25 Å, respectively, further enhancing the ligand–receptor interactions.

Fig. 9C and D showed the docking-binding mode of T3 in the active site containing the highly conserved residues Phe272, Ile275, Ile276, Ala279, Arg282, Met310, Met313, Arg316, Ala317, Leu330 Gly344, His435 and Phe455 in model 1NAX-T3 (Fig. 9C). Fig. 9D showed the –COOH group acted as the hydrogen bond acceptor, forms hydrogen bond with amino acid Arg282 (–O···HN, 1.94 Å, 145.3°) (H-1), (–O···HN, 2.10 Å, 139.4°) (H-2) and (–O···HN, 2.06 Å, 152.1°) (H-3).

In addition, dityrosine and T3 were buried in the binding pocket of the same receptor (Fig. 9E and F). We noted that the two compounds possessed the same binding site and exhibit a similar orientation, because the two compounds were structurally similar. However, there were differences existed in the structures, leading to the discrepancy of the ligand binding environment. For example, differences were observed for the two compounds in the same receptor derived from the benzene ring, caused a shift in the –COOH groups, leading to the carboxyl group of dityrosine form hydrophilic interactions with amino acid residues Arg320, Thr329, Asn331 and Gly332. Furthermore, the hydrogen bond interactions for dityrosine and T3, influence the receptor binding activity. As shown in Table 1, the two compounds displayed similar binding mode and energies (dityrosine = −10.0 kcal mol^{-1}, *T3* = −10.2 kcal mol^{-1}). Therefore, we believe that they competitively bind to the same receptor.

3.5. Dityrosine inhibits T3 binding to the TRs

Dityrosine displaced [^{125}I]T3 from endogenous TRs with an IC50 of 11.02 nM (Fig. 10A). In Fig. 10B, the Scatchard analysis revealed that addition of dityrosine decreased the association constant (K_a) from 0.0324 to 0.0213, which was expressed as the absolute value of the slope. These results suggested that dityrosine might impair thyroid hormone action by inhibiting T3 binding to the TRs.

3.6. Dityrosine down-regulates the expression of TRβ1 and its co-activator factors

Fig. 11A and B showed the down-regulation of the mRNA levels of TRs co-activator factors (*Rxrα*, *Src-1*) in dityrosine-treated cells, which also suggested that the T3-dependent activation of downstream genes are suppressed by dityrosine. Moreover, T3 treatment increases TRβ1 protein level in cells. However, this action was significantly inhibited by dityrosine (Fig. 7C and D), suggesting that the T3 transport ability and T3-dependent stimulation of downstream genes are suppressed by dityrosine.

3.7. Dityrosine suppresses TR-mediated transcription

Fig. 12 showed the activities of the four luciferases increased when cells were exposed to T3. The highest luciferase activities were observed in cells incubated with 1 μM T3. In the presence of 1 μM T3, an increasing amount of dityrosine was added to the medium, and transcriptional activity was measured. In Fig. 13, dityrosine suppressed the transcriptional activity

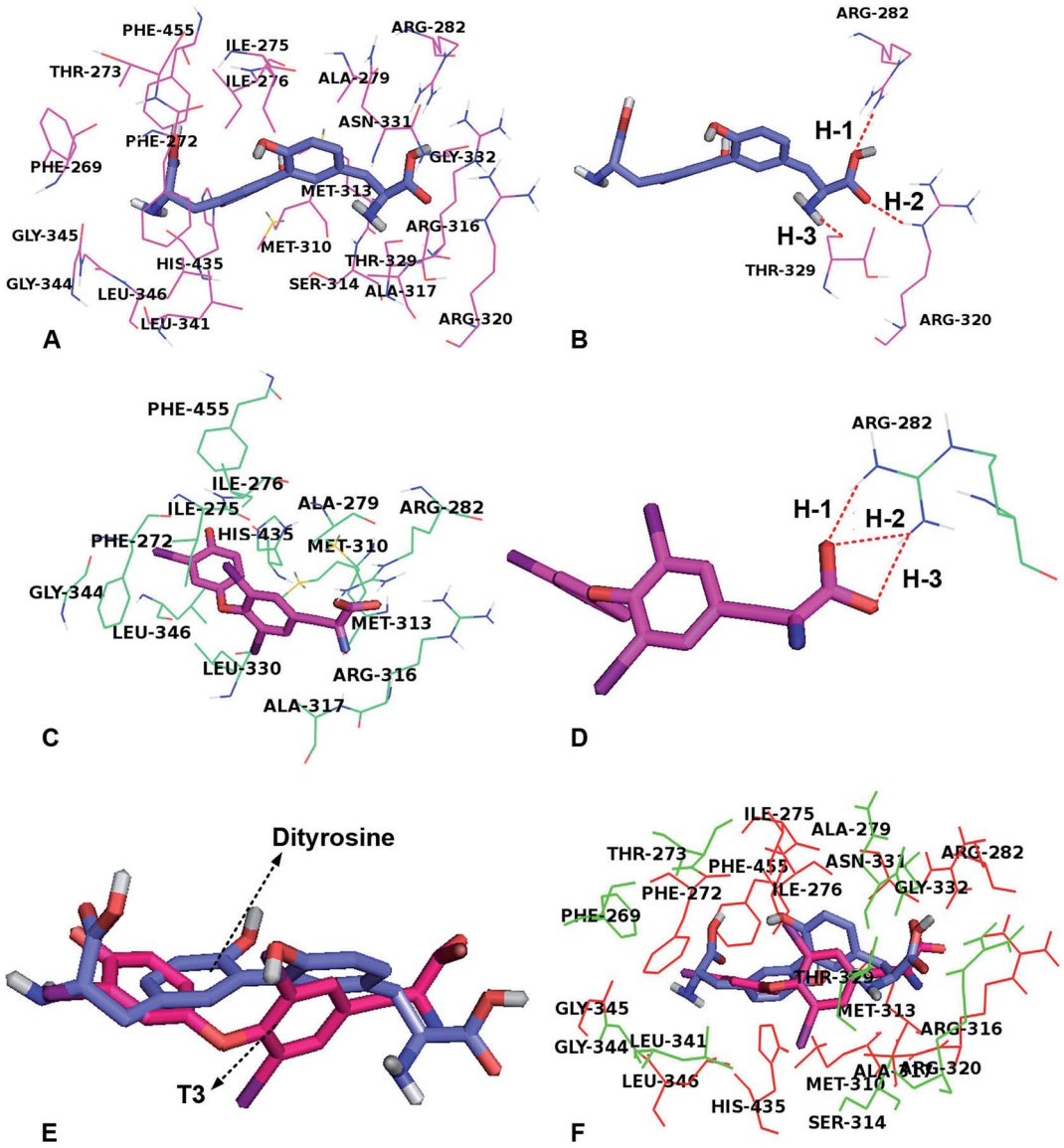

Fig. 9 Dityrosine inhibits T3 binding capacity to TRs. (A) The TRβ active site amino acid residues around dityrosine; (B) the enlargement for the ligand in the binding site after molecular docking, which is displayed in stick, hydrogen bonds are shown as dotted red lines, and the nonpolar hydrogens were removed for clarity; (C) the TRβ active site amino acid residues around T3; (D) the enlargement for the ligand in the binding site after molecular docking, which is displayed in stick, hydrogen bonds are shown as dotted red lines, and the nonpolar hydrogens were removed for clarity; (E) structural superposition of TRβ-dityrosine, TRβ-T3; (F) the amino acids located around ligands, the ligands are displayed in stick (dityrosine-blue, T3-magenta), and the related amino acids are displayed in lines (the same residues-red, different residues-green and magenta).

Table 1 The biological binding energy

Ligand–receptor	The biological binding energy
TRβ1–T3	−10.2 kcal mol^{-1}
TRβ1–dityrosine	−10.0 kcal mol^{-1}

mediated by TR in a dose-dependent manner. These results suggested that dityrosine might impair thyroid hormone action by suppressing TR-mediated transcription.

4. Discussion

Structure changes in amino acids induced by oxidation results in loss of the nutritional value and functionality of food proteins. Oxygen radicals can oxidize tyrosine residues leading to the conversion of tyrosine to 3-3′-dityrosine.[38] The structure of dityrosine is stable and does not undergo enzymatic hydrolysis easily, therefore, dityrosine is widely detected in the food system including meat and dairy products.[39,40] Dityrosine can be transported to important organs by the systemic circulation and produce harmful effects,[38,41,42] including impaired protein synthesis and cytotoxicity.[9] In this study, we observed that the liver from dityrosine-treated mice showed increased apoptosis

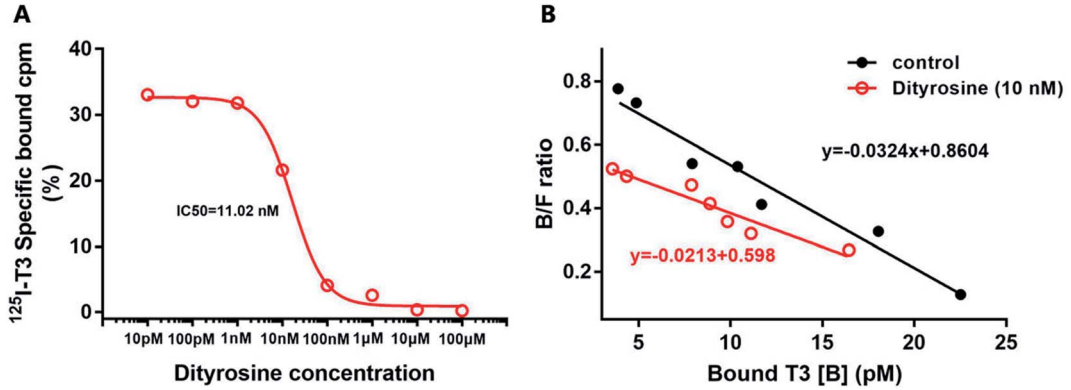

Fig. 10 (A) The inhibition binding assay. Nuclear receptor from HepG2 cell is incubated with [^{125}I] T3 and increasing amounts of dityrosine. (B) Scatchard analysis. Nuclear receptor from HepG2 cell is incubated with increasing amounts of T3 and [^{125}I] T3 in the presence or absence of dityrosine (10 nM). B, bound; F, free.

in the present of enhanced plasma THs level. It is probable that dityrosine has the potential to interfere with the cytoprotective activity of T3.

We subsequently investigated the underlying mechanism involved in the inhibition of T3 activity by dityrosine in liver. Decreased T3 transport is one plausible cause of dityrosine-dependent T3 suppression.[43] The transport of T3 into target cells requires the presence of transport proteins on the cell membrane. Monocarboxylate transporter 8 (MCT8) is a highly specific transporter of T3.[44] Decreased cellular T3 content and mRNA expression of MCT8 in dityrosine-treated HepG2 cells suggest that dityrosine inhibits T3 transport capacity in cells.

Activation of PI3k/Akt/MAPK pathway leads to events that include the triggering of the Akt kinase activation and expression of its downstream genes.[45] Herein, we show that the T3-induced anti-apoptotic effects were depressed by dityrosine, which were associated with decreased Akt activity. In addition, we also observed a key role off phosphorylated MAPK in inducing cytotoxicity during dityrosine exposure. Reports on T3 regulation of cell viability suggest that T3 is a MAPK-dependent cell growth factor.[46] In this paper, we observe that dityrosine inhibits T3-stimulated MAPK activity, which may contribute to apoptosis. MAPK is a potential upstream regulator of Bax family and its downstream caspase family members.[47] Translocation of Bax can also be regulated by the PI3k/Akt pathway,[48] and PI3k/Akt signaling promotes cell survival by up-regulating the expression of the anti-apoptotic factor Bcl-xL.[49]

The aforementioned observations demonstrate that dityrosine interferes with T3 physiological action in the process of cell survival. It has been suggested that the disruption of some

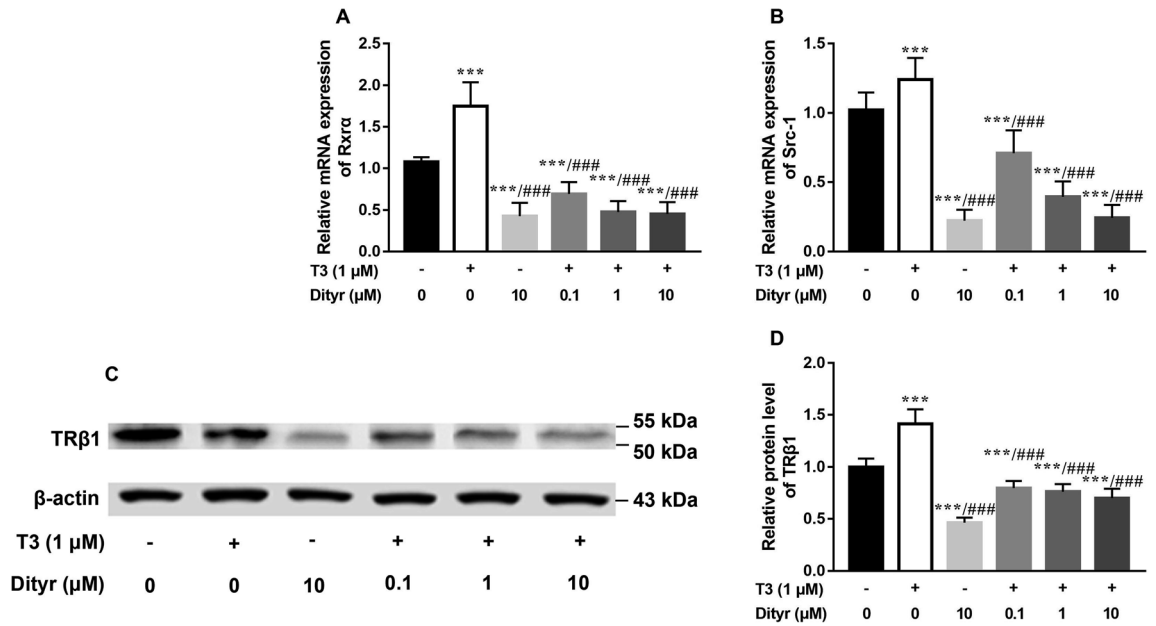

Fig. 11 Dityrosine suppresses the expression of T3 function-related factors in HepG2 cells. (A and B) The mRNA expression of Rxrα, and Src-1; (C and D) the western blot image and quantitative results of TRβ1. ***p < 0.001 when compared with the control group. ###p < 0.001 when compared with T3-only treated cells.

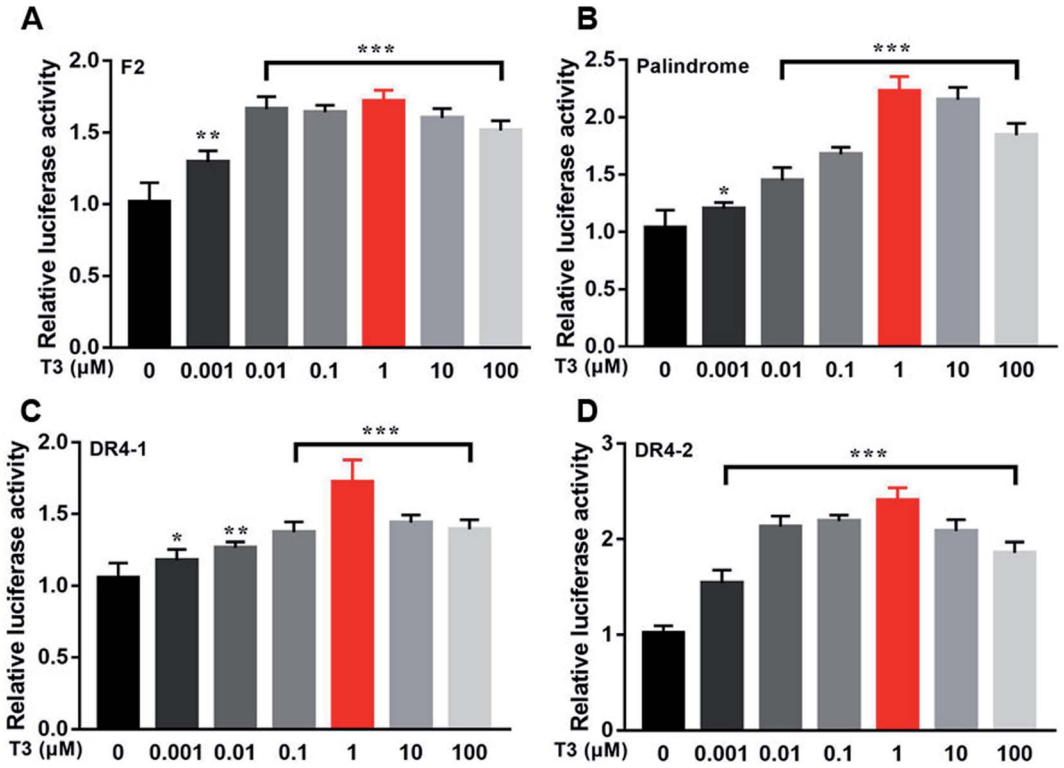

Fig. 12 The activity of the four luciferases when cells are incubated with a tracer dose of T3. ***$p < 0.001$ when compared with the control group.

industrial compounds, such as polychlorinated biphenyls (PCBs) and bisphenol A (BPA), on T3 function is thought to be due to their toxicological effects, which may be related to the structural similarities shared by PCBs, BPA and T3.[50,51] In this study, the two benzene cores are either linked by an ether bond (T3) or by a carbon-carbon bond (dityrosine). Both dityrosine and T3 molecules contain tyrosine residues. Molecular docking simulations of ligands (dityrosine and T3) binding to TRβ1 binding sites were performed in this study, which demonstrated that the two ligands were embedded into the active site with favorable poses, and the position of dityrosine in TRβ1 bore a close resemblance to that of T3, indicating that the molecular docking domain for dityrosine and T3 might be the same sites. In addition, the simulations showed that dityrosine and T3 display similar binding mode and binding energy. Therefore, we believe that these molecules bind to the same receptor in a competitive way. A novel finding from this study is that dityrosine can impair T3 action by inhibiting T3 binding to TRs and suppressing its transcriptional activity, resulting in inhibition of T3 bio-function. Suppression of T3 function is partly attributed to the inhibited T3 binding to TRs, which further suggests that dityrosine might act as an antagonist to T3.

One confounding factor which induce the disruption of T3 action may be the deficiency of thyroid hormone receptors (TRs).[52] Increasing evidence has shown that besides the classical mode of nuclear actions, TRs could act *via* extra-nuclear signaling. One important extra-nuclear pathway is mediated by PI3k signaling.[53] TRs play important roles in the regulation of cell survival *via* the PI3k pathway is first demonstrated by the finding that T3 protects pancreatic β-cells from pharmacologically induced apoptosis.[54] Subsequently, it was shown that T3-induced AKT phosphorylation is *via* TRβ1 in the rat pancreatic β-cell line (rRINm5F) and human pancreatic insulinoma cells (hCM cells).[55] This activation involves binding between the TRβ1 and the p85 submit of PI3k.[56] The binding of T3-TRs complex is located in both nuclear and cytosolic compartments to activate signaling pathways, such as MAPK and PI3k-Akt.[57–60] In the present research, dityrosine suppressed T3-dependent cytoprotection, which may be partially due to the diminished protein level of TRβ1. This, in turn would cause decreased sensitivity to T3 peripheral tissue cells.

We then quantified the luciferase activities in transgenic cells after T3 exposure in the presence or absence of dityrosine. Our results show that on adding dityrosine, the relative activity of luciferase was decreased in comparison to that of the T3 treated cells. These data explain the ability of dityrosine to modify T3-mediated effects. In addition, TRs regulate the transcriptional activity of T3 to target genes by recruitment of the 9-*cis* retinoic acid receptor (Rxr). On positive TREs, Rxr favours binding of TRs-T3 heterodimer to DNA and stimulates transcription.[61] Conformational changes of TRs induced by T3 binding release the co-repressor complex and recruit co-activators such as steroid receptor co-activator 1 (Src-1) receptors.[62,63] In this study, we observed a significant downregulation of mRNA expressions of *Rxrα* and *Src-1* in dityrosine-treated cells. These findings suggest that the dityrosine-dependent

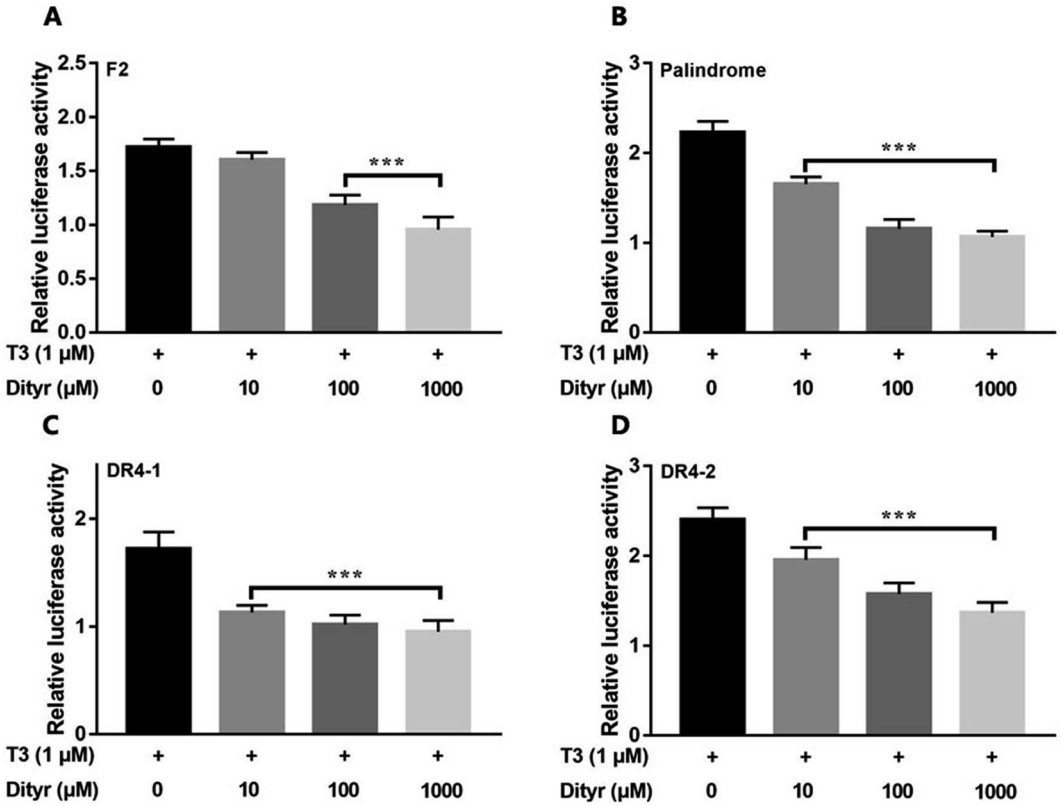

Fig. 13 The activity of the four luciferases when cells are incubated with T3 (10^{-6} M) and increasing amounts of dityrosine. ***$p < 0.001$ when compared with the control group.

decreased in cell sensitivity to T3 is also attributed to the absence of some TRs co-activator factors.

In summary, our findings demonstrate that dityrosine, which is one of the most prevalent form of oxidized tyrosine, suppresses the cytoprotective effects of T3 by inhibiting TRs-mediated transcriptional activation. Fig. 14 shows the mechanism diagram of this work, dityrosine inhibits T3 binding to TRs and downregulates its co-activator factors, which then disrupts T3-dependent PI3k/Akt/MAPK pathway activity. This study improves our understanding of the molecular mechanisms whereby dityrosine affects T3 function and establishes fundamental data for future experimental studies on dietary dityrosine. Our findings offer new light on cellular processes underlying the health threats caused by dietary oxidized protein, thus contributing to a better understanding of the diet–health axis at a cellular level.

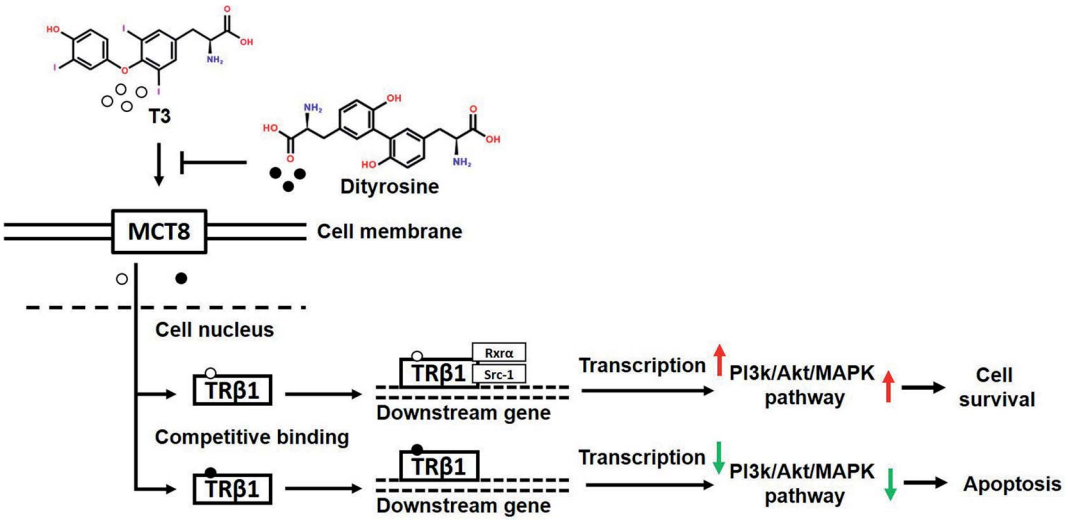

Fig. 14 The mechanism diagram of this work.

Conflicts of interest

The authorship declare no conflict of interest.

Acknowledgements

T3 binding study using [^{125}I] T3 was performed with the help of Dr Shichen Xu from Jiangsu Institute of Nuclear Medicine, Key Laboratory of Nuclear Medicine, Ministry of Health, China. This work was supported by Talent Research Start-up Foundation of Zhejiang Gongshang University 1110XJ22318010 (to Y. D.), Zhejiang Provincial Nature Science Foundation LQ19C110001 (to Y. D.), and Chinese Nature Science Foundation 31571841 (to G. L.).

References

1 Y. Y. Ding, Z. Q. Li, X. R. Cheng, Y. M. Ran, S. J. Wu, Y. Shi and G. Le, *Amino Acids*, 2017, **49**, 1401–1414.
2 M. Estévez, *Poult. Sci.*, 2015, **94**, 1368–1378.
3 M. Estevez and C. Luna, *Crit. Rev. Food Sci. Nutr.*, 2016, **57**, 3781–3793.
4 M. J. Davies, *Biochim. Biophys. Acta*, 2005, **1703**, 93–109.
5 M. A. Malik, S. N. Basahel, A. Y. Obaid and Z. Khan, *Colloids Surf., B*, 2010, **76**, 346–353.
6 Z. L. Li, L. Mo, G. Le and Y. Shi, *Food Chem. Toxicol.*, 2014, **64**, 86–93.
7 Z. Li, Y. Shi, G. Le, Y. Ding and Q. Zhao, *Oxidative Medicine and Cellular Longevity*, 2016, pp. 1–12.
8 Z. L. Li, Y. Shi, Y. Ding, Y. Ran and G. Le, *Amino Acids*, 2016, **49**, 1–20.
9 Y. Yang, H. Zhang, B. Yan, T. Zhang, Y. Gao, Y. Shi and G. Le, *J. Agric. Food Chem.*, 2017, **65**, 6957–6971.
10 Y. Yang, B. Yan, X. Cheng, Y. Ding and G. Le, *RSC Adv.*, 2017, **7**, 28591–28605.
11 Y. Y. Ding, X. R. Cheng, Z. Q. Li, S. J. Wu, Y. Yang, Y. H. Shi and G. W. Le, *RSC Adv.*, 2017, **7**, 26809–26826.
12 M. Estévez and Y. Xiong, *J. Food Sci.*, 2019, 1–10.
13 Y. Ran, B. Yan, Z. Li, Y. Ding, Y. Shi and G. Le, *Physiol. Behav.*, 2016, **164**, 292–299.
14 B. Li, Y. Ge, Y. Xu, Y. Lu, Y. Yang, L. Han, Y. Jiang, Y. Shi and G. Le, *J. Agric. Food Chem.*, 2019, **67**, 9039–9049.
15 Y. Y. Ding, X. Tang, X. R. Cheng, F. F. Wang, Z. Q. Li, S. J. Wu, X. R. Kou, Y. Shi and G. Le, *RSC Adv.*, 2017, **7**, 54610–54625.
16 A. Oetting and P. M. Yen, *Best Pract. Res., Clin. Endocrinol. Metab*, 2007, **21**, 193–208.
17 C. S. Mitchell, D. B. Savage, S. Dufour, N. Schoenmakers, P. Murgatroyd, D. Befroy, D. Halsall, S. Northcott, P. Raymond-Barker, S. Curran, E. Henning, J. Keogh, P. Owen, J. Lazarus, D. L. Rothman, I. S. Farooqi, G. I. Shulman, K. Chatterjee and K. F. Petersen, *J. Clin. Invest.*, 2010, **120**, 1345–1354.
18 E. Danforth Jr and A. Burger, *Clin. Endocrinol. Metab.*, 1984, **13**, 581–595.
19 F. C. Verga, C. Mangialardo, S. Raffa, A. Mancuso, P. Piergrossi, G. Moriggi, S. Piro, A. Stigliano, M. R. Torrisi and E. Brunetti, *Islets*, 2010, **2**, 96–103.
20 X. Cao, F. Kambe, L. C. Moeller, S. Refetoff and H. Seo, *Mol. Endocrinol.*, 2005, **19**, 102–112.
21 T. Simoncini, A. Hafezi-Moghadam, D. P. Brazil, K. Ley, W. W. Chin and J. K. Liao, *Nature*, 2000, **407**, 538–541.
22 F. C. Verga, L. Panacchia, B. Bucci, A. Stigliano, M. G. Cavallo, E. Brunetti, V. Toscano and S. Misiti, *J. Cell. Physiol.*, 2010, **206**, 309–321.
23 X. Meng, H. Wang, J. Zhao and L. Hu, *Frontiers in Oncology*, 2020, **10**, 1–13.
24 V. F. Cecilia, P. Valentina, B. Barbara, M. Claudia, M. Simona, M. Giulia, S. Antonio, B. Ercole, T. Vincenzo and M. Silvia, *J. Cell. Biochem.*, 2009, **106**, 835–848.
25 P. J. Davis, J. L. Leonard and F. B. Davis, *Front. Neuroendocrinol.*, 2008, **29**, 211–218.
26 W. M. Wiersinga, *Neth. J. Med.*, 1985, **28**, 74–82.
27 W. W. Chin and P. M. Yen, *Molecular Mechanisms of Nuclear Thyroid Hormone Action*, Humana Press, 1997.
28 V. Giguère, M. Tini, G. Flock, E. Ong, R. M. Evans and G. Otulakowski, *Genes Dev.*, 1994, **8**, 538.
29 N. Koibuchi, Y. Liu, H. Fukuda, A. Takeshita, P. M. Yen and W. W. Chin, *Endocrinology*, 1999, **140**, 1356–1364.
30 G. M. Morris, D. S. Goodsell, R. S. Halliday, R. Huey, W. E. Hart, R. K. Belew and A. J. Olson, *J. Comput. Chem.*, 2015, **19**, 1639–1662.
31 P. J. Goodford, *J. Med. Chem.*, 1985, **16**, 849–857.
32 Y. Yang, A. Zuo, Z. Zhu, X. Zhao, G. Guo and J. Zhang, *Chinese Journal of Endocrine metabolism*, 2011, 15–23.
33 O. H. Lowry, N. J. Rosebrough, A. L. Farr and R. J. Randall, *J. Biol. Chem.*, 1951, **193**, 265–275.
34 S. Shafie and S. C. Brooks, *J. Lab. Clin. Med.*, 1979, **94**, 784–798.
35 A. Baniahmad, C. Steiner, A. C. Köhne and R. Renkawitz, *Cell*, 1990, **61**, 505–514.
36 M. Tini, R. A. Fraser and V. Giguère, *J. Biol. Chem.*, 1995, **270**, 20156.
37 J. Wang, W. Xu, T. Zhong, Z. Song, Y. Zou, Z. Ding, Q. Guo, X. Dong and W. Zou, *Sci. Rep.*, 2016, **6**, 38285–38295.
38 M. E. Refaey, C. P. Watkins, E. J. Kennedy, A. Chang, Q. Zhong, K. H. Ding, X. M. Shi, J. Xu, W. B. Bollag and W. D. Hill, *Mol. Cell. Endocrinol.*, 2015, **410**, 87–96.
39 T. K. Dalsgaard, J. H. Nielsen, B. E. Brown, N. Stadler and M. J. Davies, *J. Agric. Food Chem.*, 2011, **59**, 7939–7947.
40 E. R. Stadtman, *Annual Review Biochemistry*, 1993, **62**, 797–821.
41 G. O. Hande, E. Nuran, M. Suneetha, P. Subramaniam, O. Hilmi and J. W. Heinecke, *Biochem. J.*, 2006, **395**, 277–284.
42 S. W. Chan, R. A. Dunlop, R. Anthony, K. L. Double and K. J. Rodgers, *Exp. Neurol.*, 2012, **238**, 29–37.
43 P. M. Yen, *Metabolism*, 2003, **14**, 327–333.
44 J. Bernal, *Endocrinologia y nutricion: organo de la Sociedad Espanola de Endocrinologia y Nutricion*, 2011, **58**, 185–196.
45 J. A. Fresno Vara, E. Casado, C. J. De, P. Cejas, C. Belda-Iniesta and M. González-Barón, *Cancer Treatment Reviews*, 2004, **30**, 193–204.
46 H. Y. Lin, H. Y. Tang, A. Shih, T. Keating, G. Cao, P. J. Davis and F. B. Davis, *Steroids*, 2007, **72**, 180–187.

47 R. R. Pan, C. Y. Zhang, Y. Li, B. B. Zhang, L. Zhao, Y. Ye, Y. N. Song, M. Zhang, H. Y. Tie, H. Zhang and J. Y. Zhu, *J. Nat. Prod.*, 2020, **3**, 1–11.
48 F. Tsuruta, N. Masuyama and Y. Gotoh, *J. Biol. Chem.*, 2002, **277**, 14040–14047.
49 J. Qian, Y. Zou, J. S. M. Rahman, B. Lu and P. P. Massion, *Molecular cancer therapeutics*, 2009, **8**, 101–109.
50 J. D. Mckinney, *Enviromental Health Perspectives*, 1989, **82**, 323–336.
51 M. Kenji, T. Tetsuya, A. Takashi, U. Takeshi, S. Misa, K. Naotetsu, H. Yuji, S. Akira, K. Hideshi and N. Kazuwa, *The Journal of Clinical Endocrinology*, 2002, **87**, 5185–5190.
52 X. Zhu, J. Hanover, G. Hager and S. Cheng, *J. Biol. Chem.*, 1998, **273**, 27058–27063.
53 J. W. Park and S. Y. Cheng. *SH2 Domain Structures and Interactions*, 2015, pp. 91–110.
54 F. C. Verga, E. Petrucci, V. Patriarca, S. Michienzi, A. Stigliano, E. Brunetti, V. Toscano and S. Misiti, *J. Mol. Endocrinol.*, 2007, **38**, 221–233.
55 C. V. Falzacappa, V. Patriarca, B. Bucci, C. Mangialardo, S. Michienzi, G. Moriggi, A. Stigliano, E. Brunetti, V. Toscano and S. Misiti, *J. Cell. Biochem.*, 2009, **106**, 835–848.
56 C. Liu, L. Li, H. Mei, S. Qi, P. Duan and K. Yang, *Chemosphere*, 2015, **118**, 229–238.
57 X. Mi, J. Hou, S. Jiang, Z. Liu, S. Tang, X. Liu, Y. Wang, C. Chen, Z. Wang and W. Li, *Journal of Agriculture and Food Chemistry*, 2019, **67**, 1392–1401.
58 A. D. Luca, M. R Maiello, A. D'Alessio, M. Pergameno and N. Normanno, *Expert Opinion on Therapeutic Targets*, 2012, **16**, S17–S27.
59 C. Xia, K. Fukushi, L. C. Moeller, R. Samuel and S. Hisao, *Mol. Endocrinol.*, 2005, **19**, 102–112.
60 I. Deb and S. Das, *Neurochem. Int.*, 2011, **58**, 861–871.
61 L. Laflamme, G. Hamann, N. Messier and S. Maltais, *J. Mol. Endocrinol.*, 2002, **29**, 61–72.
62 S. A. Onate, S. Y. Tsai, M. J. Tsai and B. W. Omalley, *Science*, 1995, **270**, 1354–1357.
63 Y. Hu, A. Y. Wu, C. Xu and L. H. Qiu, *Journal of Cancer*, 2019, **10**, 547–555.